Hyperfine Interactions 20(1984)249–262

THE ELECTRIC FIELD GRADIENT AT THE IRON SITES IN βFeOOH

Danny G. CHAMBAERE, Eddy DE GRAVE*, Rudy L. VANLEERBERGHE and Robert E. VANDENBERGHE

Laboratory of Magnetism, Gent State University, Proeftuinstraat 86 B-9000 Gent, Belgium

Received 27 February 1984
(Revised 17 May 1984)

The temperature behaviour of the hyperfine parameters of iron in paramagnetic chlorine containing βFeOOH is studied by ^{57}Fe Mössbauer spectroscopy. Applying external magnetic fields, the sign and asymmetry parameter η of the electric field gradient (EFG) at the compound's two iron sites is determined. It is shown that an external field enhances the distributive character of the hyperfine parameters. Finally, heat treatment experiments allow new data on the nature of both iron coordination types to be presented.

1. Introduction

The first Mössbauer measurements of the quadrupole splitting in βFeOOH date back as far as 1965 [1]. In that paper, and in several others later on, it was assumed that iron occupies only one type of octahedral O/OH coordination. In 1978, however, some of the present authors found that two discrete doublets were required to describe the paramagnetic spectra satisfactorily (fig. 6a), thus leading to the conclusion that Fe is distributed over two different types of octahedral coordination [2].

This result has since been confirmed by several researchers [3–7], although a detailed analysis of the properties of both EFG's has not been given so far, and, more important still, each author involved in the problem proposes a different hypothesis concerning the nature of the two iron surroundings. The main difficulty in identifying both iron coordinations lies with the fact that the tetragonal hollandite-like matrix of βFeOOH, proposed in 1960 by A.L. Mackay [8], implies only one obvious cation

*Research Associate at the National Fund for Scientific Research (Belgium).

site, viz. in the center of an $O_3(OH)_3$-octahedron. Throughout this work, the iron site yielding the lower quadrupole splitting will be referred to as the LD-site, while the site leading to the higher quadrupole split doublet will be referred to as the HD-site (the same letter code will be applied, either as subscript or superscript, to all physical quantities related to both sites).

In 1979 Johnston and Logan [3] suggested that the LD-doublet is caused by iron in the structural $O_3(OH)_3$ octahedron, whereas the HD-doublet arises from iron in the tunnels, i.e. the chain of cavities along the c-axis of the hollandite-like structure. Childs et al. [5] claim that protons, needed to compensate the electric charge of the Cl^- and OH^- ions in the tunnels, transform a number of normal $O_3(OH)_3$ octahedra (LD) in $O_2(OH)_4$ octahedra (HD). Ohyabu and Ujihira [6] consider normal $O_3(OH)_3$ sites (LD) and chlorine substituted octahedra such as $O_3(OH)_2Cl$ (HD). Finally, T. Mellin [7] ascribes the LD-doublet to a normal $O_3(OH)_3$ coordination and the HD-doublet to highly inhomogeneously surrounded iron in the tunnels, which he considers to be larger than usually assumed; this could be due to a possible isomorphism of certain βFeOOH zones with recently discovered manganates [9], exhibiting tunnels with a cross section of 2 by 3 (romanechite) and 3 by 3 (tokodorokite) octahedra instead of hollandite's smaller 2 by 2 tunnels.

In this paper, a detailed description of the EFG's will be presented (temperature behaviour, sign and values of the quadrupole coupling constants, asymmetry parameters), along with some annealing experiments, which shed a new light on the identity of the iron coordinations in βFeOOH.

2. Experimental techniques and data handling

The βFeOOH specimens were synthesized by hydrolysis of an $FeCl_3 \cdot 6H_2O$ aqueous solution (Weiser and Milligan's method [10]). The identification tag used in this work carries information on the synthesis circumstances; yet, this information being irrelevant to the present discussion, we refer the reader for this matter and for other structural parameters (chlorine content, crystal water content, etc.) to previous publications [11–13]. Suffice to say that all samples were characterized by X-ray diffraction (XRD) and transmission electron microscopy, and that they were all shown to be pure βFeOOH with a spindle shaped morphology.

^{57}Fe Mössbauer spectroscopy was carried out in the constant acceleration mode on a conventional spectrometer, using a ^{57}Co/Rh source and absorbers of 10 mg Fe/cm^2. External magnetic fields up to 6 T (60 kOe) were produced by a commercial superconducting system with a longitudinal field configuration, i.e. parallel to the direction of the incident γ-rays.

The externally induced magnetic interaction being of the same order of magnitude as the electric quadrupole interaction, no analytic expressions for the γ-transition energies can be obtained; in this case, the resulting spectrum is calculated by numerical

evaluation of the energy eigenvalues of the total interaction hamiltonian. We developed a suitable computer program, based on the work by Gabriel and Ruby, Collins and Travis, and F. Varret [14–16], allowing us to calculate spectra and compare them with experimental data, even in the case of a semi-continuous quadrupole interaction distribution. Thus the external field spectra presented in this paper were simulated rather than fitted, due to the considerable amount of computer time required for the theoretical shape calculations.

Isomer shifts δ are given relative to αFe at room temperature.

3. Temperature behaviour of isomer shift and quadrupole splitting

The hyperfine parameters at ambient temperature of a number of synthetic βFeOOH specimens are listed in table 1. The most striking feature is the very constancy of these quantities throughout so wide a range of investigated specimens. Even the intensity ratio of both doublets $I_{LD}:I_{HD}$ remains, within error limits, constant at 60:40.

Studying the temperature behaviour of βFeOOH's paramagnetic hyperfine parameters is forcibly confined to a rather narrow range, due to the compound's relatively high Néel temperature T_N with respect to the temperatures at which a longer stay provokes dehydration and structural changes. Therefore we selected a specimen (60A3) having one of the lowest Néel temperature (T_N = 252 K) [12], and this was studied over a range of approximately 90 K, between 255 K and 345 K. The results are graphically represented in fig. 1 and fig. 2.

The quadrupole splitting is only weakly decreasing with increasing temperature, as is to be expected for Fe^{3+}, since there is only a lattice contribution to ΔE_Q. The isomer shift δ is the sum of two contributions, the intrinsic shift δ_I and the second order Doppler shift δ_{SOD}. Considering δ_I to be temperature independent and δ_{SOD} to obey the well-known Debije approximation [17], one can determine δ_I and the Debije temperature θ_D, by a straightforward fitting procedure, in which the Debije integral involved is evaluated by series expansion [18]. This method yields only slightly different intrinsic shift values: $\delta_I^{(LD)}$ = 0.621 mm.s^{-1} and $\delta_I^{(HD)}$ = 0.613 mm.s^{-1}. Larger is the difference between both Debije temperatures: $\theta_D^{(LD)}$ = 584 K and $\theta_D^{(HD)}$ = 492 K. Temperature independence is observed for the relative intensity of both doublets and for the linewidth (FWHM) Γ_{HD}. The behaviour of Γ_{LD} is somewhat peculiar and shows that the local variation of the anion configuration constituting an LD-site is more temperature-sensitive than in the case of an HD-site.

Table 1

Isomer shift δ, quadrupole splittings ΔE_Q, linewidths Γ and fractional intensities I of both doublets in chlorine containing βFeOOH (error on ΔE_Q indicates reproducibility, on the other quantities 3 × the standard deviation of the fitting results).

Specimen	LD-doublet				HD-doublet			
	δ_{LD} (mm.s^{-1}) (±0.005)	$(\Delta E_Q)_{LD}$ (mm.s^{-1}) (±0.02)	Γ_{LD} (mm.s^{-1}) (±0.02)	I_{LD} (±0.06)	δ_{HD} (mm.s^{-1}) (±0.010)	$(\Delta E_Q)_{HD}$ (mm.s^{-1}) (±0.03)	Γ_{HD} (mm.s^{-1}) (±0.02)	I_{HD} (±0.06)
20A12	0.376	0.56	0.29	0.62	0.378	0.95	0.32	0.38
20A24	0.376	0.55	0.30	0.64	0.380	0.93	0.32	0.36
40A64	0.372	0.52	0.27	0.59	0.378	0.92	0.30	0.41
60A1.5	0.373	0.53	0.30	0.60	0.379	0.94	0.34	0.40
60A3	0.369	0.54	0.31	0.59	0.377	0.94	0.34	0.41
60A17	0.371	0.52	0.28	0.59	0.378	0.92	0.32	0.41
60A50	0.371	0.52	0.27	0.58	0.377	0.93	0.30	0.42
80A1.5	0.372	0.53	0.28	0.62	0.378	0.92	0.32	0.38
80A4	0.371	0.51	0.28	0.57	0.377	0.92	0.32	0.43
80A8	0.370	0.52	0.29	0.59	0.376	0.93	0.32	0.41
80A19	0.370	0.53	0.27	0.60	0.376	0.92	0.30	0.40
80A50	0.372	0.52	0.27	0.57	0.379	0.93	0.30	0.43
100A1.5	0.373	0.52	0.28	0.58	0.380	0.93	0.31	0.42
100A5	0.373	0.54	0.27	0.58	0.379	0.96	0.30	0.42

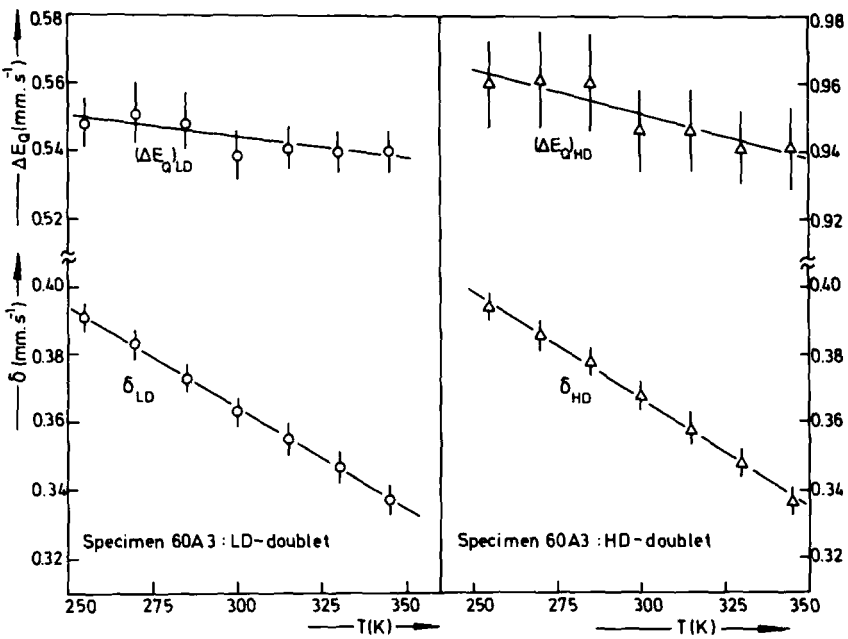

Fig.1. Isomer shift δ and quadrupole splitting ΔE_Q of βFeOOH as a function of temperature. Full lines: ΔE_Q: least-squares straight line; δ: Debye model fitting (see text).

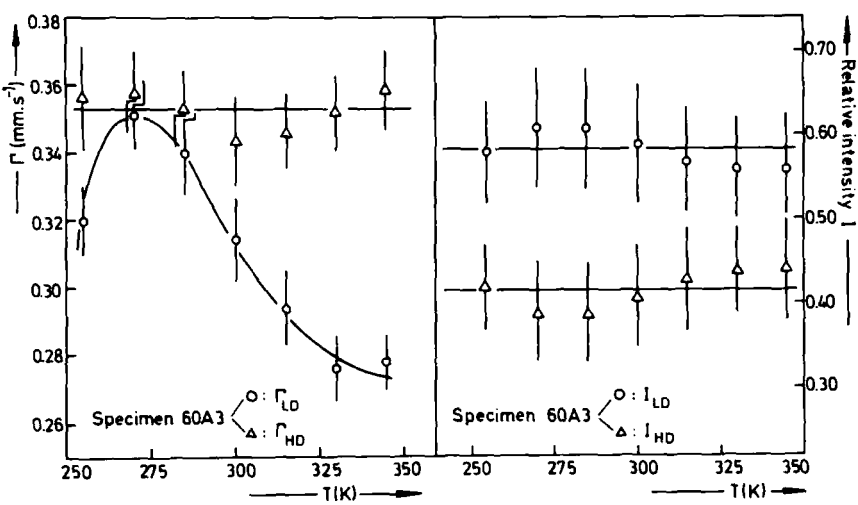

Fig. 2. Linewidths Γ and fractional intensities of both doublets as a function of temperature. (Full lines as a guide for the eye.)

4. Sign and asymmetry of both EFG's

4.1. SOME PRELIMINARY REMARKS AND EXPERIMENTS

The external field measurements and the simulation procedure leading to the sign of the quadrupole coupling constant e^2qQ (i.e. the sign of V_{zz}, the largest component of the diagonalized EFG tensor), and to the asymmetry parameter η of that tensor ($\eta = (V_{xx} - V_{yy})/V_{zz}$, with $|V_{zz}| > |V_{yy}| > |V_{xx}|$) were carried out on only one specimen, 60A17.

It is well known that nuclei of a paramagnet in an external field H_{ex} do not feel the exact strength of that field, due to ionic spin polarization, which sets up a second contribution to the effective field H_{eff}; the magnetic hyperfine interaction in ^{57}Fe being negative, this results in a field reduction with respect to the external field. C.E. Johnson [19] showed that this phenomenon leads to an effective field at the iron nucleus given by:

$$H_{eff} = H_{ex}\left(1 - \frac{\chi H_0}{Ng\mu_B S}\right). \tag{1}$$

χ is the magnetic susceptibility per mass unit, H_0 the saturation hyperfine field, N the number of magnetic dipoles per mass unit, g the Landé splitting factor, μ_B the Bohr magneton, and S the 3d-spin value.

The external field measurements were performed at 302 K; from earlier Faraday susceptibility measurements and stoichiometrical reasoning [11 – 13], we are able to derive χ at 302 K ($27.03\ 10^{-6}$ cm^3/g), N ($5.86\ 10^{21}$ g^{-1}) and S (1.83).

A series of low temperature Mössbauer experiments ($T < 60$ K) allowed the evaluation of H_0 by extrapolation to absolute zero. With the two types of iron coordination, LD and HD, correspond two H_0-values; in the case of specimen 60A17 this yields: $H_0^{(LD)} = 477.4$ kOe and $H_0^{(HD)} = 491.0$ kOe. The third sextet contribution previously observed in βFeOOH [4,5], was found to be thermally generated, and to disappear at absolute zero within the experimental error limits ([11] and submitted to J. Magn. Magn. Mat.). So H_0 in eq. (1) is evaluated as the weighted mean value of $H_0^{(LD)}$ and $H_0^{(HD)}$, using the relative occurrence of both coordinations as listed in table 1:

$$H_0 = I_{LD}\, H_0^{(LD)} + I_{HD}\, H_0^{(HD)} = 483 \text{ kOe} . \tag{2}$$

Since $g = 2$ for the S-state Fe^{3+} ion, we are able to calculate the effective field from eq. (1). Field reduction due to spin polarization thus amounts to 6.6% in βFeOOH (60A17).

Next to H_{eff} other parameters are needed to calculate the shape of the spectra: linewidths Γ, isomer shifts δ, quadrupole splittings ΔE_Q and intensities I, though, are

known from zero field measurements (table 1), so that the only variables left in the simulation procedure are η and the sign of e^2qQ; indeed, the numerical value of e^2qQ is fixed once an η-value is chosen, since ΔE_Q is known, and the three quantities are linked by the expression:

$$\Delta E_Q = \left|\frac{e^2qQ}{2}\right| \left(1 + \frac{\eta^2}{3}\right)^{1/2} . \tag{3}$$

4.2. EXTERNAL FIELD MEASUREMENTS AND QUALITATIVE INTERPRETATION

Figure 3 shows the evolution of the Mössbauer spectrum of paramagnetic βFeOOH in an increasing magnetic field: the doublet broadens and then turns into a three-line-structured spectrum (because of its apparent shape, further referred to as 'triplet').

Simulations have shown that at relatively low field strengths (e.g. 12 kOe), spin polarization effects and influences of η on the spectrum shape are negligible, so that an eventually occurring intensity asymmetry in the broadened doublet must be entirely due to the sign of the EFG. Fig. 4 shows a simulation of a βFeOOH spectrum at 12 kOe with both $(e^2qQ)_{LD}$ and $(e^2qQ)_{HD}$ chosen positive, resulting in the right-hand side peak being deeper than the left-hand side one; this picture is simply reversed for two negative e^2qQ-values. Since no such intensity asymmetry is observed in the 12 kOe experimental spectrum (fig. 3), both EFG's in βFeOOH must have opposite signs. Under these circumstances, simulations of 45 kOe and 60 kOe spectra (fig. 3 and fig. 5) show that the marked shape asymmetry in the central triplet line (broadened to the left-hand side) can only be realized if $(e^2qQ)_{LD}$ is positive and $(e^2qQ)_{HD}$ is negative.

The determination of η_{LD} and η_{HD} is more difficult, because their influence on the global spectrum is far less than that of a sign reversal. Nevertheless, even at this stage, simulations reveal the following points:

(1) None of the iron coordinations have an axial symmetric EFG.

(2) The agreement between the outer flanks of the simulated and the experimental spectrum is practically entirely determined by the effective field; e.g. taking no field reduction into account results in a quite obvious bad agreement (fig. 5a). The best agreement, though, is indeed obtained by using the 6.6% field reduction based on a 3d-spin of 1.83 (fig. 5b); this corroborates the earlier reported unusually large spin reduction in βFeOOH, shown to be the fundamental reason for the behaviour of the compound's Néel temperature and other magnetic properties [11,12].

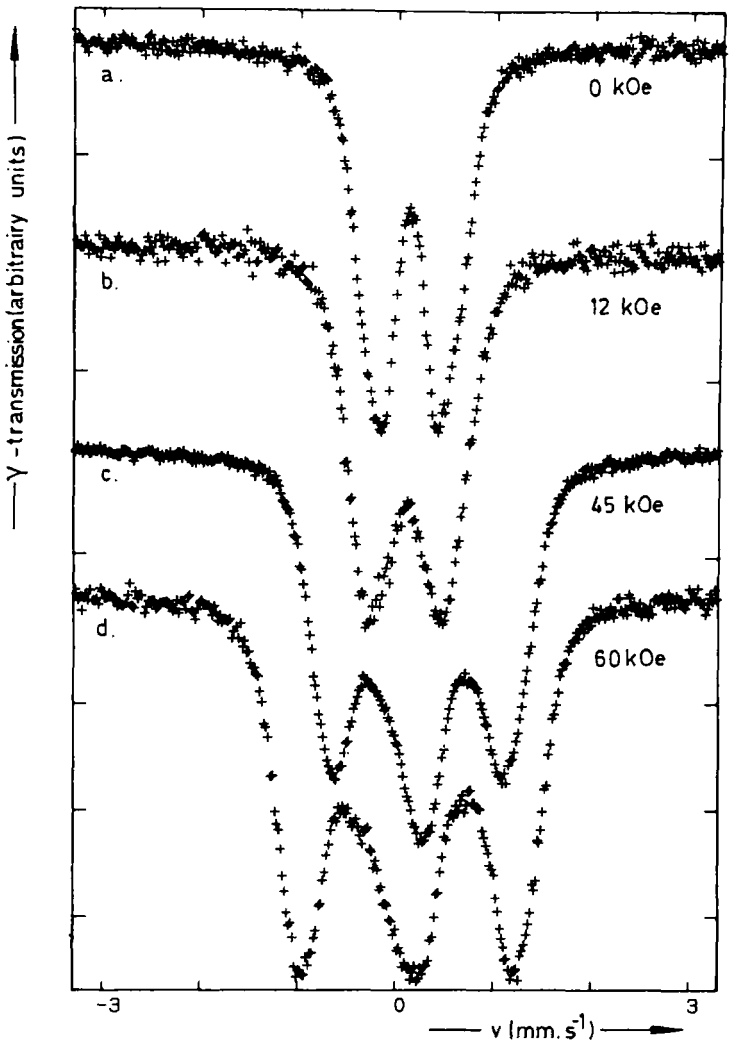

Fig. 3. Paramagnetic chlorine containing βFeOOH in an increasing external magnetic field (specimen 60A17 at 302 K).

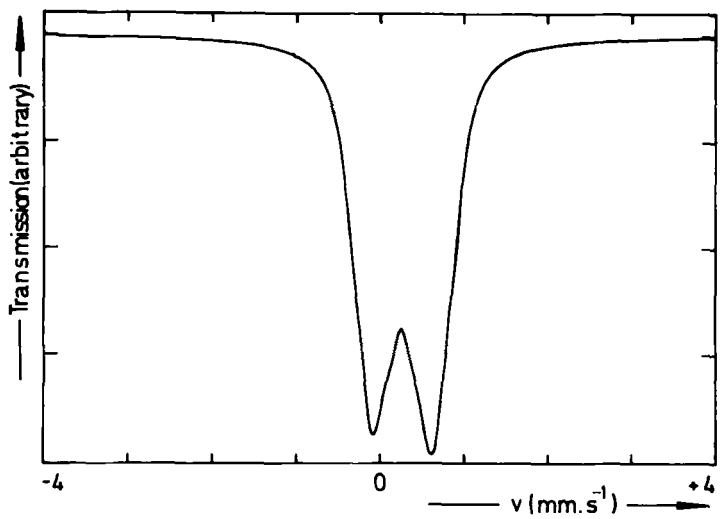

Fig. 4. Simulation of βFeOOH spectrum at 12 kOe using two positive EFG's.

4.3. A SEMI-CONTINUOUS APPROACH: QUADRUPOLE INTERACTION DISTRIBUTIONS

Even after profuse simulation work, no calculated spectrum better than the one represented in fig. 5b could be obtained. In an attempt to eliminate the remaining discrepancies, a more continuous approach to the problem was made: instead of describing the local quadrupole splitting variation within each type of coordination by a simple broadening of the lorentzian lines (cfr. Γ's of 60A17 in table 1), the explicit form of this distribution was introduced in the calculations: the zero field spectrum was analyzed with a finite sum of lorentzian contributions, all having the instrumental width (0.25 $mm.s^{-1}$).

To this end we designed a computer program based on the method proposed by Wivel and Mörup [20]. The results are shown in fig. 6b and 6c; the latter figure represents the obtained quadrupole *splitting* distribution (histogram). In addition to evidence from the derivative of the βFeOOH Mössbauer spectrum, this semi-continuous analysis proves that there are only two 'main' sites in chlorine containing βFeOOH [21]. Since we had already found that we are actually dealing with EFG's of opposite sign, this purely mathematical quadrupole *splitting* distribution was separated into two physically relevant quadrupole *interaction* distributions by fitting two gaussian profiles to the global distribution function (full lines in fig. 6c).

This procedure shows that both approaches, i.e. the discrete one using only two (broadened) doublets (fig. 6a), and the semi-continuous one using a distribution

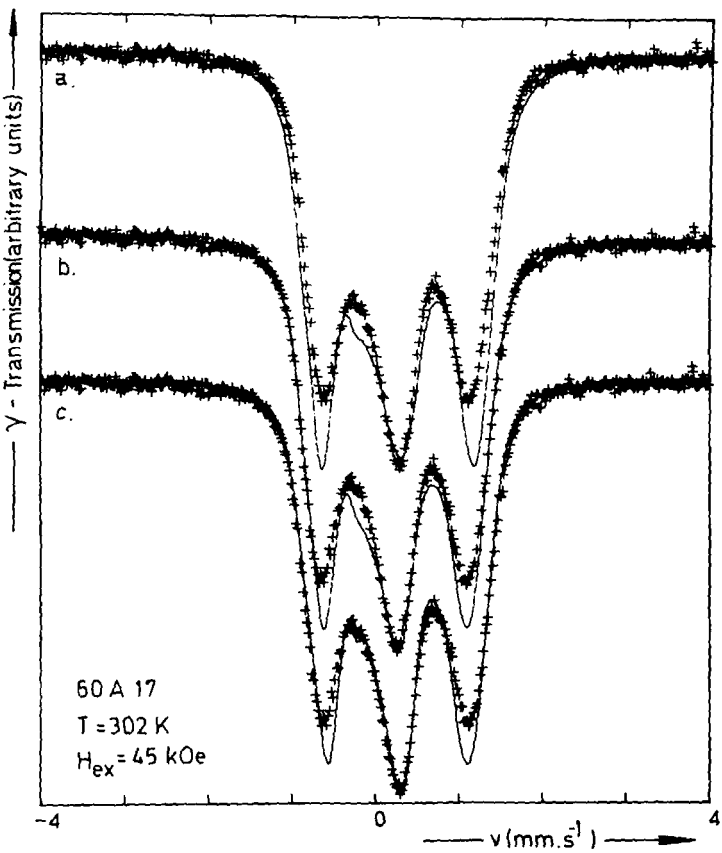

Fig. 5. Simulations (full lines) of the 45 kOe experimental spectrum of paramagnetic βFeOOH:
(a) best simulation without field reduction;
(b) best simulation using a 6.6% field reduction (see text);
(c) optimum simulation using the same field reduction as in (b) and a distribution of quadrupole interactions.

(fig. 6b), are completely equivalent in the absence of an external field: the top of the LD-distribution lies at 0.51 mm.s^{-1}, that of the HD-distribution at 0.95 mm.s^{-1} (discrete case: 0.52 mm.s^{-1} and 0.92 mm.s^{-1}, respectively); the fractional areas of the corresponding gaussian distribution functions are I_{LD} = 0.59 and I_{HD} = 0.41, i.e. exactly the same values as obtained by the discrete analysis of 60A17 (table 1).

A different situation arises when an external field is applied: the introduction of a quadrupole interaction distribution definitely improves the agreement between simulation and experiment, especially in the central part of the triplet (fig. 5c).

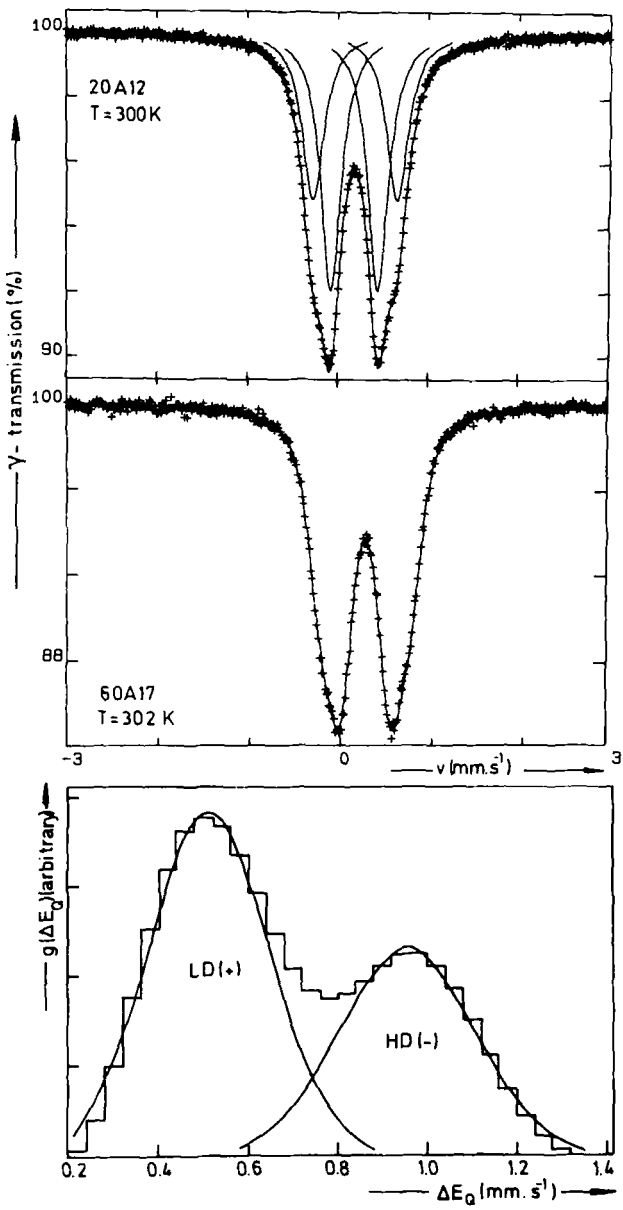

Fig. 6. (a) βFeOOH spectrum fitted with two discrete doublets;
(b) βFeOOH spectrum fitted with a semi-continuous distribution of doublet contributions;
(c) resulting quadrupole splitting distribution (histogram) and separation in two gaussian quadrupole interaction distributions (full line) of opposite sign (see text).

Yet, there remains a discrepancy in the relative intensities of the calculated triplet lines. In our opinion, this could only be eliminated by taking the distributive character of the other quantities involved into account as well: indeed, as we have shown in an earlier paper [12], βFeOOH exhibits a distribution of several magnetic properties, induced by a variable amount of crystal water, so that the effective field will be varying throughout the sample; also, since V_{zz} is distributed, so must V_{xx} and V_{yy}, and hence η be, because they are linked by Laplace's equation. Yet, taking all this explicitly into account would exponentially enhance computational complexity and time demands up to an unrealistic level. Fig. 5c thus represents the best simulation obtained; the deduced properties of βFeOOH's EFG are listed in table 2.

Table 2

EFG characteristics of both iron sites in βFeOOH (| |: uncertainty interval)

	LD coordination	HD coordination
$\frac{e^2qQ}{2}$ (mm.s^{-1})	+0.49 |+0.45, +0.52|	−0.84 |−0.79, −0.90|
η	0.6 | 0.5, 0.75 |	0.8 | 0.7, 0.9 |

One general conclusion might perhaps be drawn: in Mössbauer spectroscopy, the distributive character of certain hyperfine parameters, which in zero field spectra can be perfectly accounted for by a slight broadening of the lorentzian lines, manifests itself more obviously and requires a far more detailed approach, even beyond feasibility, when an external magnetic field is switched on.

5. On the nature of both coordination types

In order to monitor the evolution with temperature of βFeOOH's dual iron coordination, we have carried out isochronous heating experiments. To this end, two specimens were selected, strongly different in crystal water content x_{H_2O}, i.e. the number of interstitial water molecules per unit cell [11 – 13]. Several batches of each were heated under ambient atmospheric circumstances for 15 minutes at increasingly higher temperatures T_h, and Mössbauer spectra at room temperature of the resulting products were subsequently recorded. Fig. 7 represents the evolution of the fractional

doublet intensity of both coordinations. At higher temperatures a third coordination type arises (referred to as 3D), but by then the structure is highly degenerated into a quasi-amorphous state and this phenomenon, being of no concern to the present discussion, will be thoroughly treated in another paper (manuscript in preparation). At

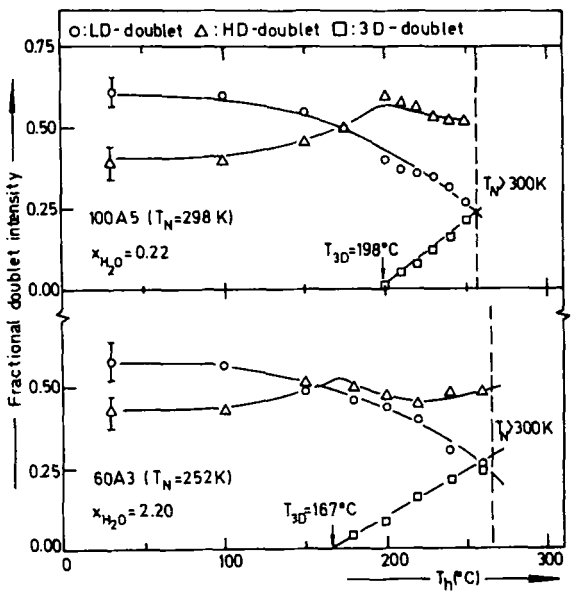

Fig. 7. Behaviour of the fractional doublet intensities as a function of the isochronous heat treatment temperatures T_h for 2 βFeOOH specimens. (Full lines through I_{LD} and I_{HD} points as a guide for the eye.)

lower temperatures though, XRD shows that no considerable structural changes take place and yet we observe for each specimen a decrease of the LD-contribution in favour of the HD-contribution as the heating temperature T_h is raised.

One may have noticed that all the hypotheses concerning the nature of the iron coordinations, which we cited in the introduction, have one feature in common: they all consider the LD-doublet to arise from iron surrounded by a normal $O_3(OH)_3$ anion configuration. Now in our opinion, the observation that with increasing T_h the number of LD-surroundings decreases, is difficult to reconcile with the generally proposed $O_3(OH)_3$ nature of the anion octahedron responsible for the LD-doublet. This would indeed mean that the most stable, structural anion configuration changes itself in one of the 'other' coordination types mentioned in the introduction, involving rather unlikely phenomena such as migration of iron to the tunnels (in the case of [3]

and [7]), or increasing OH substitution by chlorine (in the case of [6]), or increasing proton density in the lattice (in the case of [5]).

Therefore, we are inclined to favour the mechanism proposed by Childs et al. [5], though with a reversed doublet assignment, i.e. the LD-doublet corresponding to an $O_2(OH)_4$ octahedron and the HD-doublet to an $O_3(OH)_3$ octahedron. Our experiments can then be explained in the following way: when heated, Cl^- and/or OH^- ions leave the structure, thus reducing the number of charge compensating protons and hence decreasing the number of $O_2(OH)_4$ coordinations (responsible for the LD-doublet) by transforming them back into $O_3(OH)_3$ octahedra (responsible for the HD-doublets).

Acknowledgements

The authors are grateful to the Belgian Foundation FKFO for financial support and to the Director of the Laboratory of Magnetism, Professor Dr. G. Robbrecht, for his continuous interest in our work.

References

[1] M. Rossiter and A. Hodgson, J. Inorg. Nucl. Chem. 27(1965)63.
[2] D. Chambaere, A. Govaert, J. De Sitter and E. De Grave, Solid State Commun. 26(1978)657
[3] J.H. Johnston and N.E. Logan, J. Chem. Soc. Dalton Trans. 13(1979)13.
[4] E. Murad, Clay Minerals 14(1979)273.
[5] C. Childs, B. Goodman, E. Paterson and F. Woodhams, Aust. J. Chem. 33(1980)15.
[6] M. Ohyabu and Y. Ujihira, J. Inorg. Nucl. Chem. 43(12)(1981)3125.
[7] T. Mellin, Doctoral Thesis, University of Göteborg, Sweden (1981).
[8] A.L. Mackay, Mineralogical Mag. 32(1960)545.
[9] S. Turner and P. Buseck, Science 212(1981)1024.
[10] H. Weiser and W. Milligan, J. Phys. Chem. 39(1935)25.
[11] D. Chambaere, Doctoral Thesis, Gent State University, Belgium (1983).
[12] D. Chambaere and E. De Grave, J. Magn. Magn. Mat. 42(1984)263.
[13] D. Chambaere and E. De Grave, Phys. Stat. Solidi (a) 83(1)(1984)93.
[14] K. Gabriel and S. Ruby, Nucl. Instrum. Meth. 36(1965)23.
[15] R. Collins and J. Travis, in: *Mössbauer Effect Methodology,* Vol. 3, ed. I.J. Gruverman (Plenum Press, New York, 1967) p. 123.
[16] F. Varret, J. Phys. Colloq. C6 37(1976)437.
[17] R.V. Pound and G.A. Rebka, Jr., Phys. Rev. Lett. 4(1960)250.
[18] S. Heberle, in: *Mössbauer Effect Methodology,* Vol. 7, ed. I.J. Gruverman (Plenum Press, New York, 1971) p. 299.
[19] C.E. Johnson, Proc. Phys. Soc. 92(1967)748.
[20] C. Wivel and S. Mörup, J. Phys. E 14(1981)605.
[21] R. Vanleerberghe and Ph. Van Acker, Nucl. Instrum. Meth. 206(1983)339.